General Disclaimer

One or more of the Following Statements may affect this Document

- This document has been reproduced from the best copy furnished by the organizational source. It is being released in the interest of making available as much information as possible.

- This document may contain data, which exceeds the sheet parameters. It was furnished in this condition by the organizational source and is the best copy available.

- This document may contain tone-on-tone or color graphs, charts and/or pictures, which have been reproduced in black and white.

- This document is paginated as submitted by the original source.

- Portions of this document are not fully legible due to the historical nature of some of the material. However, it is the best reproduction available from the original submission.

N O T I C E

DEVELOPMENT OF A VALIDATION MODEL

FOR THE

DEFENSE METEOROLOGICAL SATELLITE PROGRAM'S

SPECIAL SENSOR MICROWAVE IMAGER

C. T. Swift and M. A. Goodberlet

University of Massachusetts

Amherst, MA 01003

J. C. Wilkerson

NOAA/NESDIS

Suitland, MD 20016

November 18, 1990

Abstract

As part of a subcontract with the manufacturer of the Defense Meteorological Space Program's (DMSP) Special Sensor Microwave/Imager (SSM/I), an operational wind speed algorithm was developed by Environmental Research & Technology Inc. (ERT). The ERT algorithm is based on the "D-matrix" approach which seeks a linear relationship between measured SSM/I brightness temperatures and environmental parameters. D-matrix performance was validated by comparing algorithm derived wind speeds with near-simultaneous and co-located measurements made by off-shore ocean buoys maintained by the National Oceanic and Atmospheric Administration. The DMSP accuracy requirement of $\pm$ 2 m/s for wind speed predictions in the range of 3 m/s to 25 m/s was not obtainable with the original version of the D-matrix which had severe bias and scaling problems. Revisions to the algorithm made at the University of Massachusetts caused it to perform within specifications. Other topics include, error budget modeling, alternate wind speed algorithms, and D-matrix performance with one or more inoperative SSM/I channels.

1. Introduction

The Defense Meteorological Space Program (DMSP) Special Sensor Microwave/Imager (SSM/I) wind speed retrieval algorithm developed by Environmental Research and Technology, Inc. (ERT) under contract from Hughes Aircraft is called the D–matrix algorithm and has the following form [Lo, 1983].

$$SW = C0(j)+C1(j){\cdot}TB(19H)+C2(j){\cdot}TB(22V)+C3(j){\cdot}TB(37V)+C4(j){\cdot}TB(37H) \quad (1)$$

Equation (1) is valid only over open ocean where the wind speed, SW, is in m/s and referenced to a height of 19.5 m above the surface. Equation (1) also contains the terms TB(x) which represent the SSM/I measured brightness temperature of frequency/polarization combination "x" and the D–matrix coefficients, Ci(j), where "j" is the climate code index and varies from 1 to 11. The eleven sets of coefficients (only 9 of which are distinct) used in the original D–matrix algorithm are given by Lo [1983]. Each of the 9 distinct climate codes represents a particular season and latitude band as shown in Table 1.

The amount of microwave energy being emitted from the ocean surface is dependent on the wave structure and foam coverage [Ulaby et al., 1986a] which are, in turn, influenced by the ocean surface wind speed. Therefore, by measuring the ocean surface microwave emission, the SSM/I is able to predict ocean surface wind speed. Microwave emission at the SSM/I frequencies which is coming from the ocean surface is effectively masked by the emission and attenuation characteristics of the rain and large amounts of water vapor in the earth's atmosphere. Realizing this, ERT suggested the use of a rain–flag which attempts to identify conditions under which less accurate wind speed retrievals are produced. The original rain–flag logic is shown below.

	Season	Climate
Zone	(Northern Hemisphere)	Code
Tropics	JUN–NOV	1
(0–20 LAT.)	DEC–MAY	2
Low Lat. Transition	JUN–NOV	3
(20–25 LAT.)	DEC–MAY	4
Mid–Latitude	SEP–NOV, MAR–MAY	5
(25–55 LAT.)	JUN–AUG	6
	DEC–FEB	7
ARCTIC	MAY–OCT	8
(55–90 LAT.)	NOV–APR	9

Table 1. Climate codes of the Hughes D–matrix algorithm.

IF: TB(19H) > 190K

OR: $|TB(37V) - TB(37H)| < 25K$

Then possible rain exists and rain-flag = 1

IF: $|TB(37V) - TB(37H)| < 10K$

Then heavy rain exists and rain-flag = 2

Otherwise rain-flag = 0

The DMSP accuracy specification for wind speed retrievals under rain-free conditions (i.e., rain-flag = 0) was ± 2 m/s (standard deviation) over the range 3 m/s to 25 m/s. Accuracy was not specified for wind retrievals from cells flagged either 1 or 2. In fact, the original D-matrix algorithm did not attempt to retrieve winds under rain-flag 2 conditions.

2. NOAA Buoy System and Criteria for Comparison

Validation of the SSM/I wind speed retrievals was done using the anemometer measured winds of open ocean buoys maintained by the National Oceanic and Atmospheric Administration (NOAA). These buoys make an 8.5 minute average of the wind once every hour with an accuracy of ± 0.5 m/s for winds less than 10 m/s and 5% for winds greater than 10 m/s [Gilhousen, 1986a].

To prevent land contamination of ocean brightness temperatures and to insure that the land did not restrict the wind speed fetch distance necessary for creating fully developed seas [Ulaby et al, 1986b], only buoys further than 100 km from land were chosen for the validation. The 19 NOAA buoys used for the validation are listed in Table 2, each of which makes speed measurements at heights of either 5 or 10 meters above the surface. These measurements were converted to equivalent winds at 19.5 meters above the surface

Buoy I.D.	Latitude	Longitude (E)	Zone	SSM/I Overpasses in 30 Days
51002	17.2	202.2	Tropics	31
51004	17.5	207.4	Tropics	31
51003	19.2	199.2	Tropics	32
51001	23.4	197.7	Low Lat Trans	33
42001	25.9	270.3	Mid Lat	33
42002	26.0	266.5	Mid Lat	33
42003	26.0	274.1	Mid Lat	33
41006	29.3	282.6	Mid Lat	34
41002	32.2	284.7	Mid Lat	35
44004	38.5	289.4	Mid Lat	38
46006	40.8	222.4	Mid Lat	39
44011	41.1	293.4	Mid Lat	40
46002	42.5	229.6	Mid Lat	41
44005	42.7	291.7	Mid Lat	41
46005	46.1	229.0	Mid Lat	43
46004	50.9	224.1	Mid Lat	47
46003	51.9	204.1	Mid Lat	48
46001	56.3	211.7	Arctic	55
46035	57.0	182.3	Arctic	56

Table 2.   NOAA buoys used for the SSM/I wind speed validation.

[Liu et al., 1984] so that they could be compared directly to the D matrix estimates which are also referenced to 19.5 meters above the surface. Converted buoy winds and D-matrix winds were paired only when the SSM/I retrieval was located within 25 km of the buoy position and the SSM/I overpass time was within 30 minutes of the buoy wind speed measurement. Based on the work of Monaldo [1988], the average values of these spatial and temporal differences increases the total standard deviation of 2 m/s by less than 10%; a small contribution to the overall error. Because a 25 km spatial separation introduces little additional error to the comparison of SSM/I and buoy winds, the SSM/I geolocation problem [Hollinger et al., 1988] which results in positioning errors of between 5 and 25 kilometers, does not significantly affect the wind speed validation. Several of the wind speed retrievals associated with each SSM/I overpass of the buoy may meet the comparison criteria, however, such a set of retrievals are highly correlated with each other. In an attempt to assemble a collection of independent SSM/I-buoy comparisons, only one retrieval from each SSM/I overpass is used.

3. Required Number of Comparisons

The accuracy specification of ± 2 m/s for D-matrix wind speed retrievals can be interpreted in at least two ways. One interpretation is that this is the standard deviation, in an average sense, of the difference between all coincident buoy and SSM/I wind speed measurements. An alternative interpretation is that the standard deviation of such comparisons in any sub-interval of the 3-25 m/s wind speed range must not exceed 2 m/s. The first of these two interpretations can disguise the fact that over certain sub-intervals of the 3-25 m/s wind speed range, the accuracy of the D-matrix prediction may be worse than ± 2 m/s. A modeled error budget predicts that this will be true as discussed

in section 4. It is possible that sub-intervals with accuracies worse than ± 2 m/s could average with sub-intervals having accuracies better than ± 2 m/s to give a resulting overall accuracy of better than ± 2 m/s. This is often true for regression-type algorithms, like the D-matrix, which tend to make especially good predictions near the overall average wind speed and predictions of less accuracy for wind speeds which are removed from the average wind speed.

For these reasons, the 3-25 m/s wind speed range of interest was divided into the 6 sub-intervals shown in Table 3 and the D-matrix performance was analyzed in each sub-interval. Also shown in Table 3 are the number of comparisons out of 1,000 for which the buoy wind speed falls within the particular sub-interval range. These comparison counts are based on the global distribution of winds given by Schroeder et al. [1986] which is shown in Figure 1.

It is preferable to have a sample size of 30 or more when doing statistical analysis of the data. For wind speed sub-intervals 1, 2, and 3, it appears that this sample size can be obtained by collecting approximately 140 comparisons. Preliminary studies showed that about 15% of the data are rain-flagged and since the comparisons are made only with data which is not rain-flagged, the sample size required for each climate code needed to be increased 15% from 140 to 161. Although the time between successive SSM/I overpasses of a buoy depends on the buoy's latitude, 161 comparisons could be obtained in 60 days using only three buoys. Other factors which affect the total required buoy count, include lost data due to periodic buoy maintenance, missing SSM/I data, and the likelihood of encountering wind speeds distributed according to Figure 1 [Schroeder et al., 1986]. These factors were determined from actual climatic summaries for the individual data buoys which are available from the National Data Buoy Center [Gilhousen et al., 1986b]. The

| | Comparisons | |
I.D.	Range (m/s)	per 1000
1	3-6	260
2	6-10	395
3	10-14	215
4	14-18	50
5	18-22	25
6	22-25	1

Table 3. Expected number of D-matrix/buoy wind speed comparisons per 1000 which fall into selected subintervals of the 3 m/s to 25 m/s wind speed range.
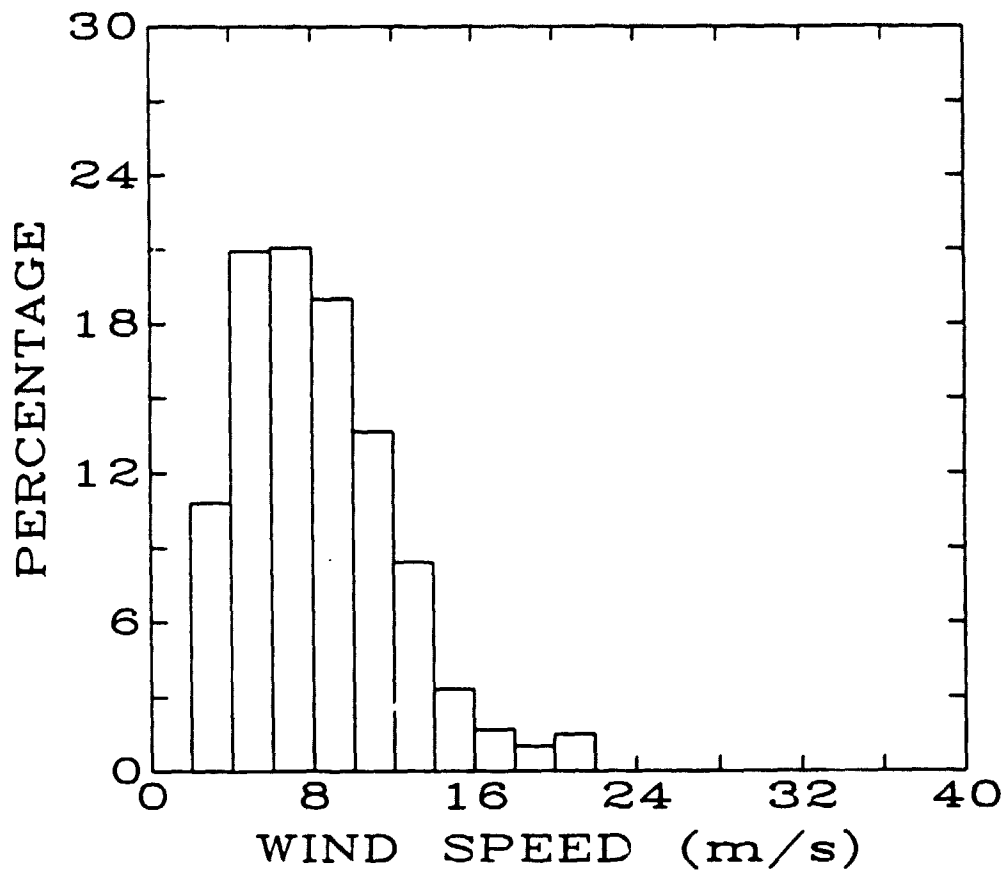
Figure 1.   The global distribution of ocean surface winds [Schroeder and Sweet, 1986].

climatic summaries established that the 19 buoys selected could more than satisfy the low wind speed validation requirements. However, the low probability of observing winds greater than 15 m/s makes it difficult to evaluate the overall performance of the D-matrix algorithm in the range 15-25 m/s. This problem is discussed with more detail in section 6.

4. Pre-Launch Validation Modeling — Error Budget

The sources of random errors associated with the comparison of SSM/I wind retrievals and converted ocean buoy measurements are summarized in the following error budget.

* Extrapolation noise. (Buoy averaging time at a point differs from the instantaneous spatial average made by the SSM/I)

* SSM/I instrument noise.

* Buoy instrument noise.

* D-matrix algorithm model noise. (D-matrix algorithm's inability to model exactly the radiative transfer processes)

* Decorrelation noise. (Spatial and temporal separation of the SSM/I and buoy measurements)

* Translation noise. (Errors in translating the buoy wind measurement to a height of 19.5 m)

* Round-off noise. (Error due to the nearest m/s round-off of the SSM/I retrieved wind speeds)

The magnitude of these errors less decorrelation noise and translation noise is shown in Figure 2 over the wind speed range of 3 m/s to 25 m/s for the climate code 5 algorithm. Plots for the other 8 versions of the D-matrix algorithm are very similar to the results of
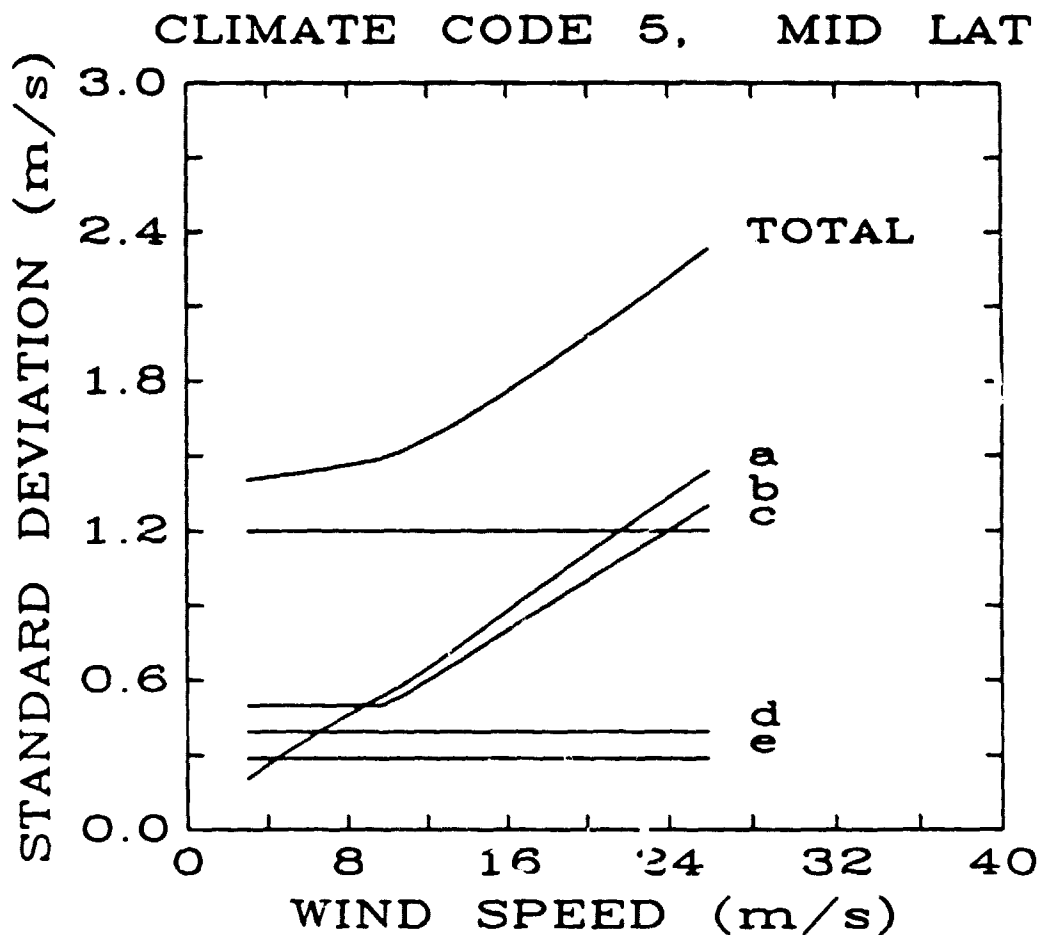
Figure 2.   Random errors affecting D-matrix wind speed retrievals from climate code 5. Shown are the standard deviations of the errors due to (a) extrapolation noise, (b) buoy instrument noise, (c) D-matrix algorithm model noise, (d) SSM/I instrument noise, and (e) D-matrix retrieval round-off noise.

climate code 5 and are therefore not shown. In generating the extrapolation noise curve of Figure 2, the one-dimensional wind field model of Pierson [1983] was used as were effective footprint diameters for the 19, 22, and 37 GHz SSM/I channels of 55, 49, and 32 km, respectively. The buoy noise, which was discussed previously, is from Gilhousen [1986a]. The model noise was specified in a report by Hughes Aircraft [1980].

The instrument noise as specified by Hollinger et al. [1987] for the SSM/I channels of 19H, 22V, 37V, and 37H is 0.41, 0.75, 0.38, and 0.39 degrees Kelvin, respectively. The round-off noise is due to the fact that the operational D-matrix algorithm results are rounded off to the nearest whole m/s before being archived. Although the round-off noise does not contribute significantly to the total error of D-matrix retrievals, subsequent users of the data can cause a "double rounding" error when converting from the D-matrix values (in m/s) to either miles/hour or knots and then again rounding to the nearest whole number. In the case of converting to knots, the "double rounding" average error is 0.7 knots but can be as large as 1.5 knots. The average errors due to spatial and temporal separation of SSM/I and buoy measurements are not included in the plot since they do not contribute significantly to the total. Likewise, errors in converting the buoy wind measurements to a height of 19.5 m are insignificant and are not shown in the plot.

Throughout this report, we assume that the buoy measures the "true" wind speed and that the difference between this measurement and that of the SSM/I is due solely to SSM/I inaccuracies. However, one should realize that our choice of the "true" wind speed is somewhat arbitrary and that the buoy, as well as the act of comparing spatially and temporally averaged winds, contribute to the total error of the comparison. In this light, one can calculate the portion of the comparison error which is attributable only to the

SSM/I from the curves in Figure 2 which correspond to D matrix algorithm model noise and SSM/I instrument noise.

5. Validation Results

Performance of the climate code 5 version of the original D-matrix algorithm is shown by the scatter-plot in Figure 3. The legend associated with the scatterplot is interpreted as follows. The bias and slope data indicates the y-axis intercept and slope of the regression line, which has been chosen to minimize the sum of the squares of the _horizontal_ distances from each point to the regression line. The SD is the standard deviation of the quantity, (D-matrix winds minus buoy winds). The term "CORR(R)" is the correlation coefficient [Book, 1977] between buoy winds and D-matrix winds. Finally, the term "#OBS" represents the number of observations or data points in the scatterplot. Figure 3 indicates that the climate code 5 D-matrix wind speed retrievals are scaled and biased by 0.85 and 5.7 m/s, respectively. This poor performance of the climate code 5 algorithm is typical of the other versions of the original D-matrix algorithm. To correct this problem new coefficients were generated using standard linear regression of buoy wind speed on the coincident SSM/I brightness temperature measurements, TB(19H), TB(22V), TB(37V), and TB(37H). Performance of the new climate code 5 D-matrix algorithm is shown in Figure 4. The regression line associated with this scatter-plot now has the desired slope of 1.0 and bias of 0.0 indicating that the scale and bias problems of the original algorithm have been corrected. Despite the apparent good performance of the new algorithms, additional improvements are necessary and will be discussed in section 6.

Before analyzing the retrieval accuracy over various wind speed sub-intervals, it was necessary to re-evaluate the rain-flag criteria. New rain-flag thresholds were determined

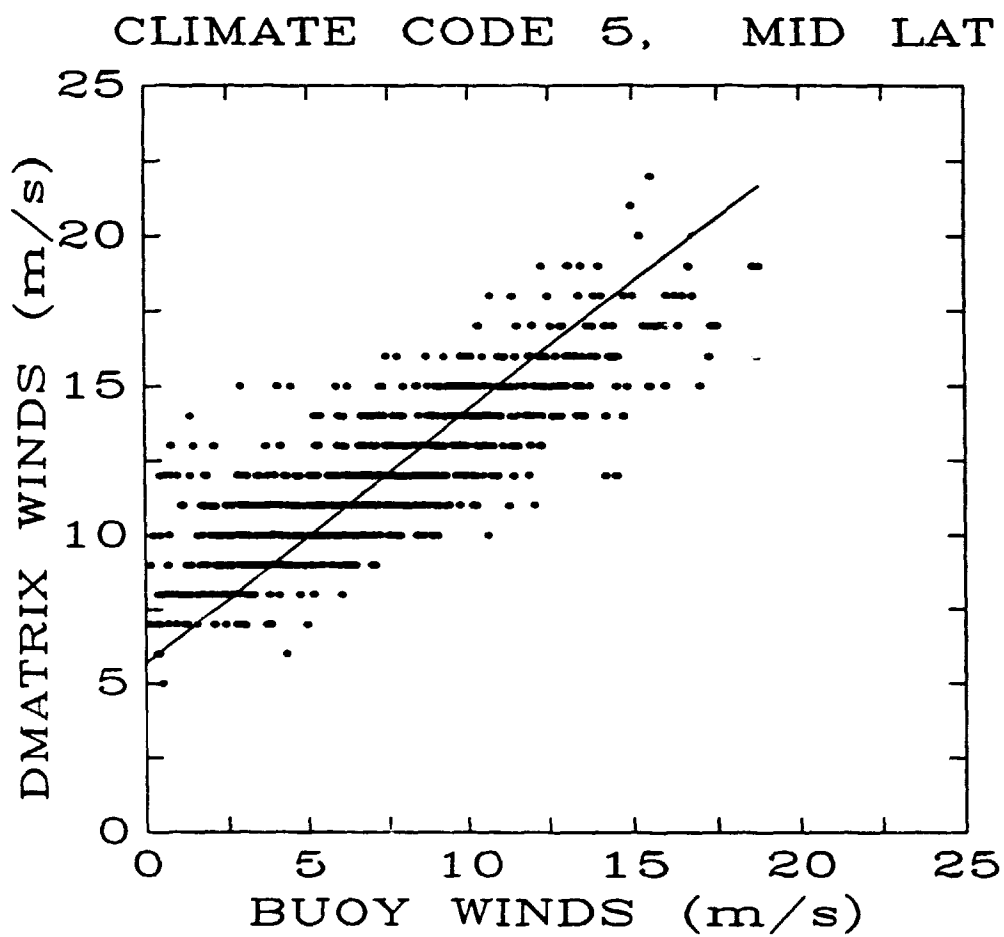CLIMATE CODE 5,   MID LAT

Figure 3.   Performance of the original D-matrix algorithm for climate code 5. Bias =

5.7 m/s, slope = 0.85, S.D. = 5.1 m/s, corr (R) = 0.82, # obs = 998.
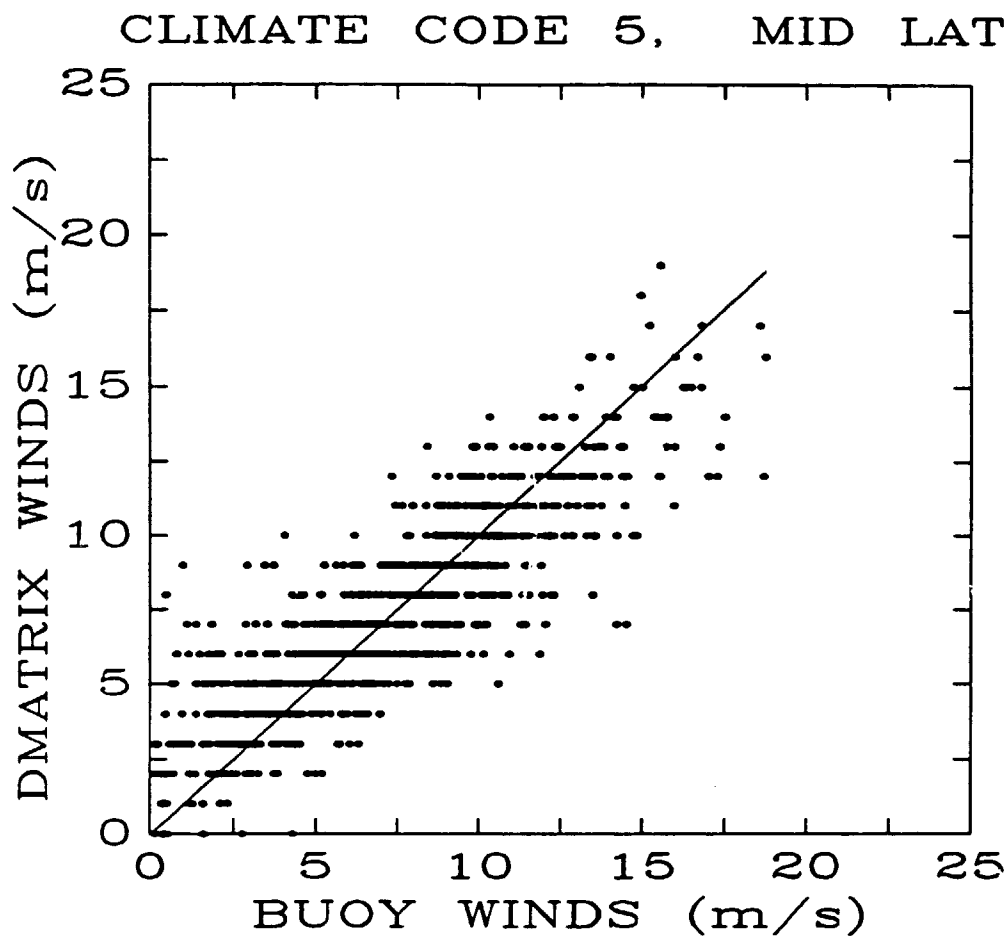
Figure 4.   Performance of the revised D-matrix algorithm for climate code 5. Bias = 0.0 m/s, slope = 1.0 m/s, S.D. = 1.9 m/s, corr (R) = 0.85, # obs = 998.

using residual plots like those shown in Figures 5 and 6 which indicate the performance of the new D-matrix algorithm as a function of the parameters used to determine rain which are $(TB(37V) - TB(37H))$ and $TB(19H)$. Each of the residual plots were then divided into a number of vertical bins and the standard deviation, SD, and average (also called bias) of the points falling within each bin were calculated. The results of these calculations are shown in Figures 7 and 8. The rain-flag cutoffs were determined from the plots by locating the values of the rain-flag parameters for which either the "SD" or "BIAS" curves crossed some predetermined accuracy level. For example, the accuracy requirement for retrievals tagged with rain-flag zero is 2 m/s. From Figures 7 and 8, one can see that the algorithm fails to meet this specification when either $(TB(37V) - TB(37H)) < 50$ or TB(19H) > 150. In this way, four entirely new rain-flags were defined (see Table 4.) which differ significantly in both number and meaning from the three ERT rain-flags. It is recommended that wind speeds be calculated under all conditions and that the accuracy associated with these new rain-flags be the user's guide to the accuracy of the retrieval. Finally, we point out that the term "rain-flag" is somewhat misleading since the rain-flag tags indicate any condition (including rain) which leads to reduced retrieval accuracy. The D-matrix retrievals are, in fact, very sensitive to rain since rain rates of less than 1 mm/hr will trip rain-flag 1 [Hollinger, et al., 1988].

Shown also in Table 4 are the new D-matrix coefficients which were derived using actual SSM/I data from the period 10 July 1987 through 31 March 1988. The measured standard deviation of the difference between buoy winds and D-matrix winds for each of the 9 climate codes under rain-flag 0 conditions is shown in Table 5. At least in the average sense, all 9 D-matrix algorithms appear to exceed the accuracy specification of ±
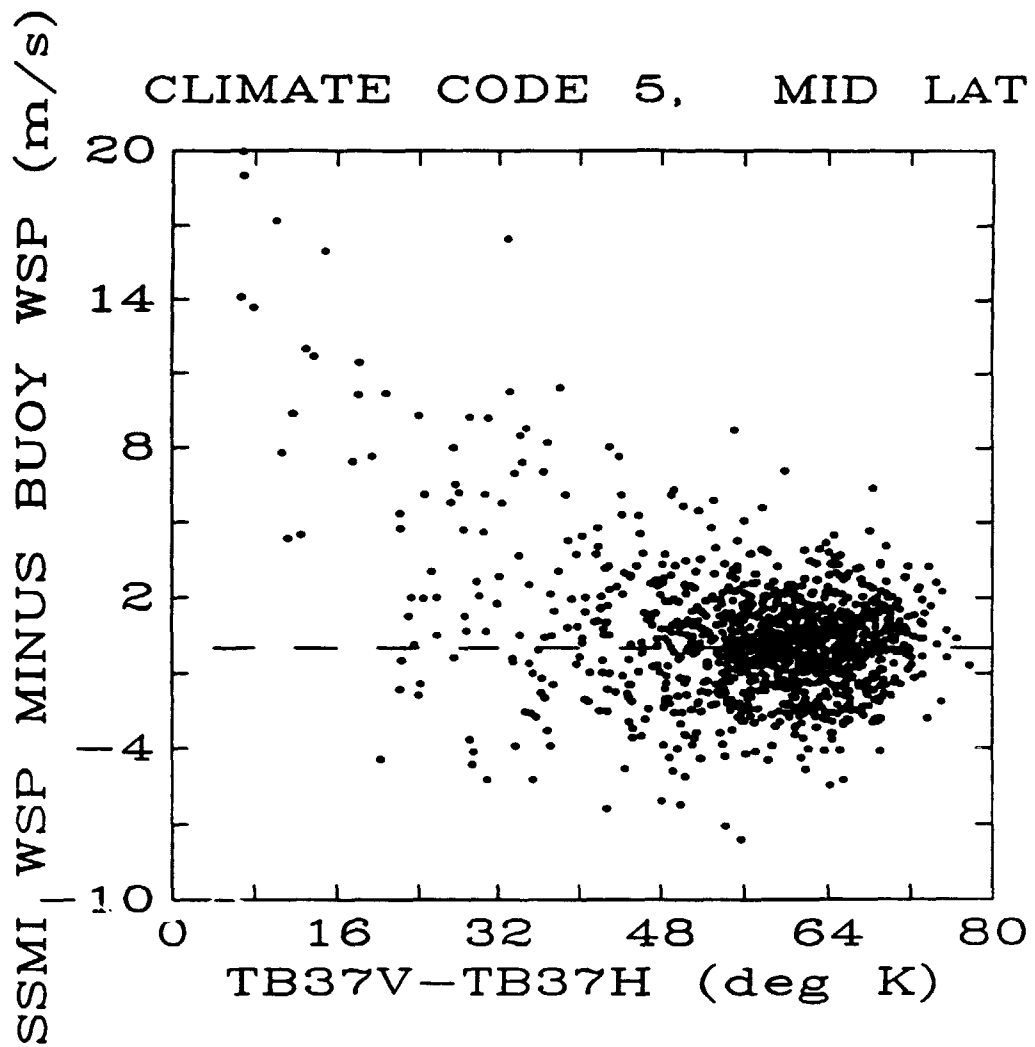
Figure 5.   D-matrix residual plotted as a function of the rain-flag, $(TB37V - TB37H)$, for climate code 5.
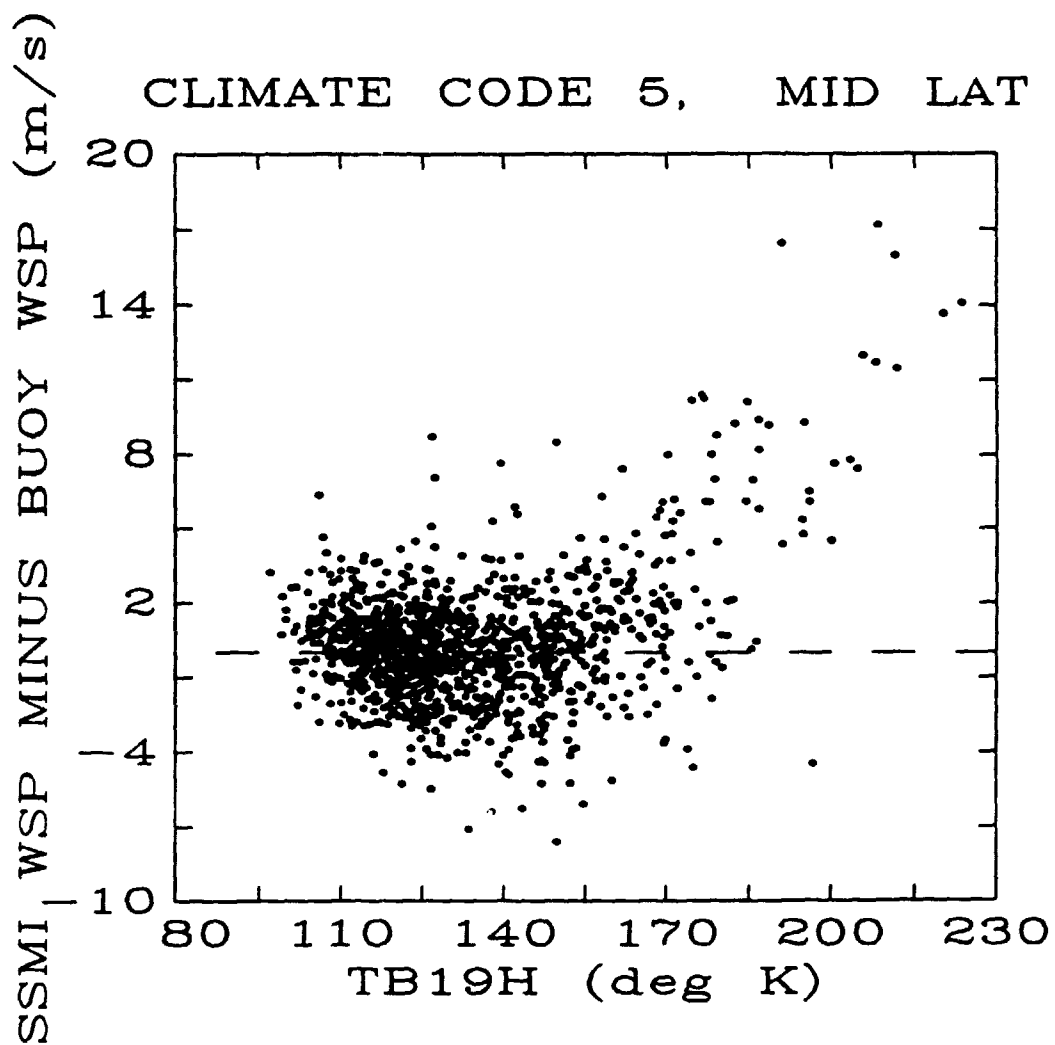
Figure 6.   D-matrix residual plotted as a function of the rain-flag, TB19H, for climate
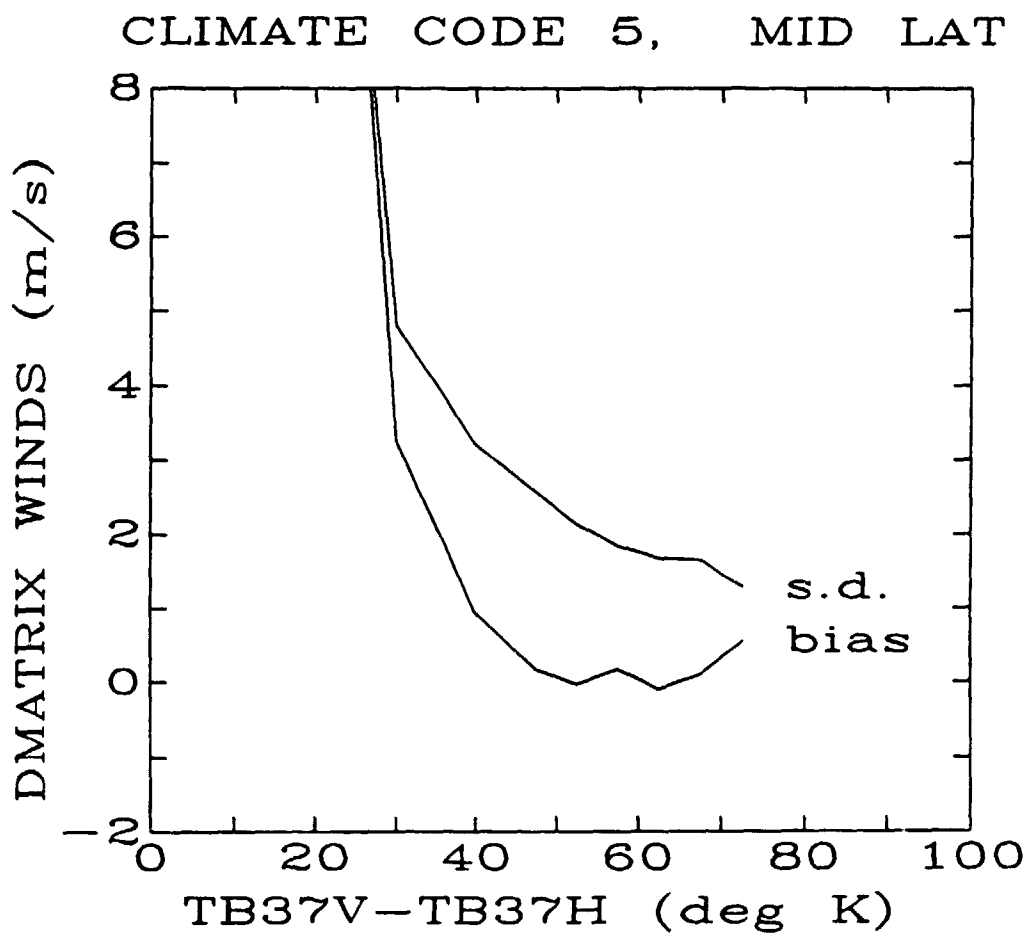
code 5.

Figure 7. Standard deviation and bias of the D-matrix retrieved winds plotted as a function of the rain-flag. ($TB37V - TB37H$), for climate code 5.
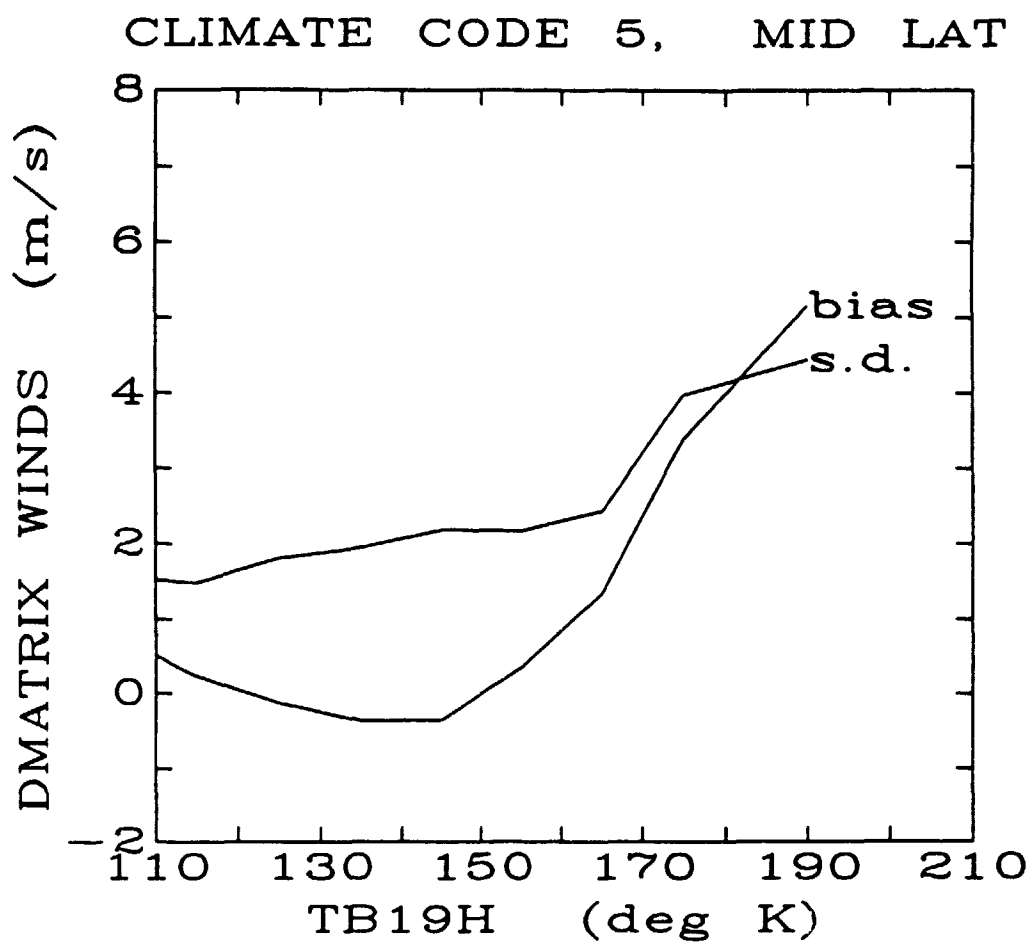
CLIMATE CODE 5, MID LAT

Figure 8.   Standard deviation and bias of the D-matrix retrieved winds plotted as a function of the rain-flag, $TB19H$, for climate code 5.

$$SW = C_0 + C_1 \cdot T_B(19H) + C_2 \cdot T_B(22V) + C_3 \cdot T_B(37V) + C_4 \cdot T_B(37H)$$

Rain Flag	Criteria	Accuracy
0	$(T_B(37V) - T_B(37H)) > T_0$ and $T_B(19H) < T_1$	$< 2\ m/s$
1	$(T_B(37V) - T_B(37H)) < T_0$ or $T_B(19H) > T_1$	$2 - 5\ m/s$
2	$(T_B(37V) - T_B(37H)) < T_2$	$5 - 10\ m/s$
3	$(T_B(37V) - T_B(37H)) < T_3$	$> 10\ m/s$

Climate Code	C_0	C_1	C_2	C_3	C_4	T_0	T_1	T_2	T_3
1	211.22	0.5090	−0.3703	−1.1944	0.4458	50	175	25	20
2	202.87	0.1316	−0.2455	−1.3138	0.8080	50	175	25	20
3	195.18	0.2996	−0.2363	−1.2266	0.5776	50	175	25	20
4	172.72	0.3908	−0.3130	−1.0396	0.4926	50	175	25	20
5	158.63	0.4224	−0.2439	−0.9839	0.3725	50	165	30	25
6	161.45	0.2964	−0.1613	−1.0632	0.4524	50	165	30	25
7	151.04	0.5991	−0.3274	−0.9137	0.2977	50	165	30	25
8	137.72	0.7330	−0.4208	−0.7533	0.1804	50	130	35	30
9	109.93	0.8695	−0.4710	−0.6008	0.1158	50	130	35	30

Table 4. New rain-flag criteria and coefficients for the 9 climate code D-matrix algorithm.

Climate Code	S.D., m/s	Percentage Rain Flagged	Number of Comparisons
1	1.5	17	376
2	1.4	10	63
3	1.5	8	109
4	1.5	9	43
5	1.8	13	1296
6	1.5	12	643
7	1.9	18	516
8	1.8	19	279
9	1.6	9	277

Table 5.   Performance of the 9 climate code D-matrix algorithm.

2 m/s. Also shown in Table 5 is the percentage of wind retrievals tagged with a rain flag of 1 or higher and the number of buoy/D-matrix wind comparisons.

Although the results shown in Table 5 are quite good, the D- matrix wind speed algorithm has several limitations which are discussed in the following section.

6. D-Matrix Limitations

Plotting the D-matrix wind speed residual as a function of buoy measured wind speed demonstrates the D-matrix performance over sub-intervals of the 3-25 m/s range. Figure 9 shows the plot for climate code 5 which is typical of all 9 climate code versions of the D-matrix. Dividing the region of Figure 9 into a number of vertical bins and calculating the SD and bias (i.e., average) of the points falling within each bin results in the "interpreted" residual plot shown in Figure 10. Figure 10 indicates that the accuracy of the D matrix retrievals is best near the global average wind speed of 7 m/s and becomes worse for predictions away from 7 m/s. Note that the SD curve trend agrees quite well with the pre-launch error budget model described in Figure 2. Also note from the bias curve of Figure 10 that the high wind speed (>15 m/s) retrievals are biased low by more than 2 m/s.

Discontinuity of the retrieved winds across climate code boundaries is another problem with the 9-version D-matrix algorithm. The average discontinuity across each latitude band boundary was calculated using actual SSM/I data and the results are summarized in Table 6. Though usually within the ± 2 m/s DMSP specification, these zonal boundary discontinuities can exceed 2 m/s in the high wind regions surrounding typhoons and hurricanes, making the study and forecasting of these storms difficult.
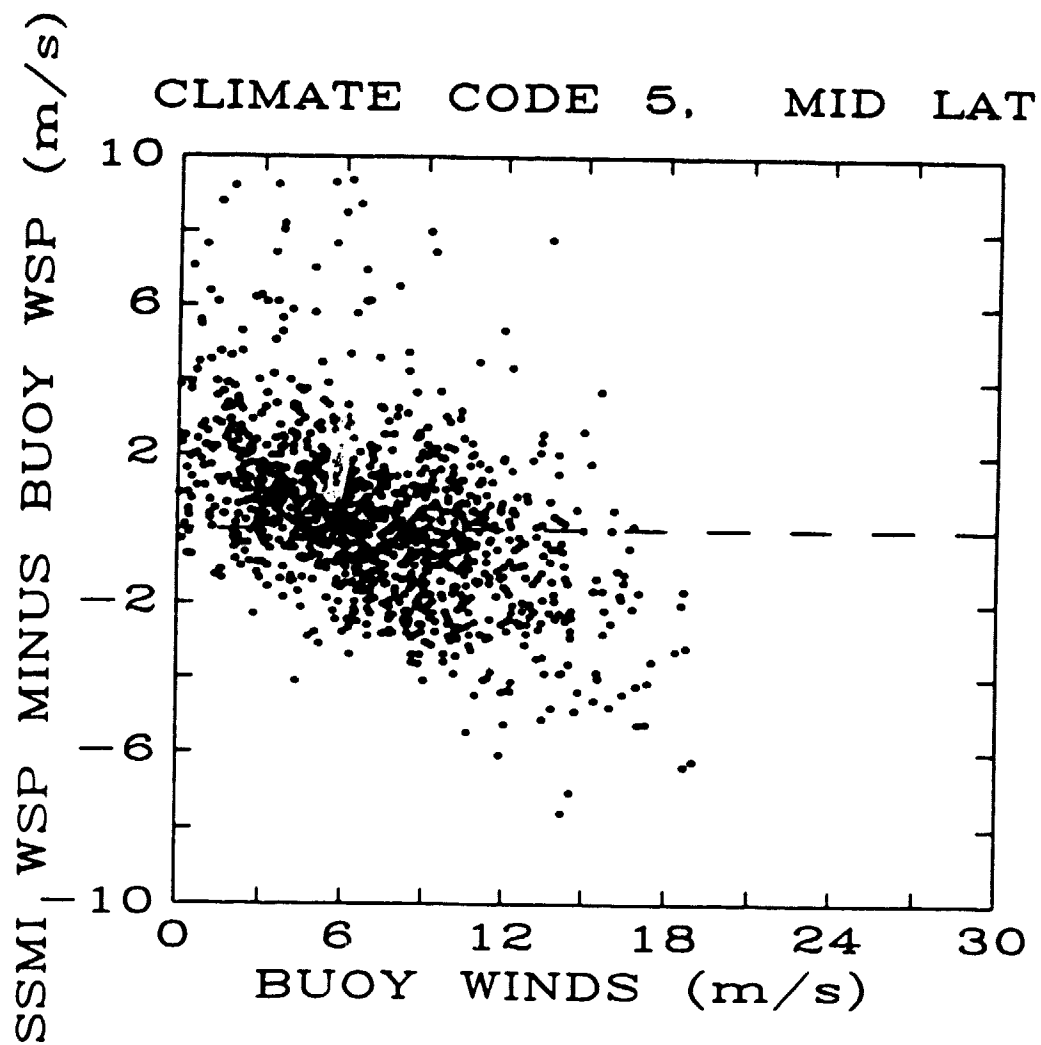
Figure 9.   D-matrix residual plotted as a function of the coincident buoy winds for climate code 5.
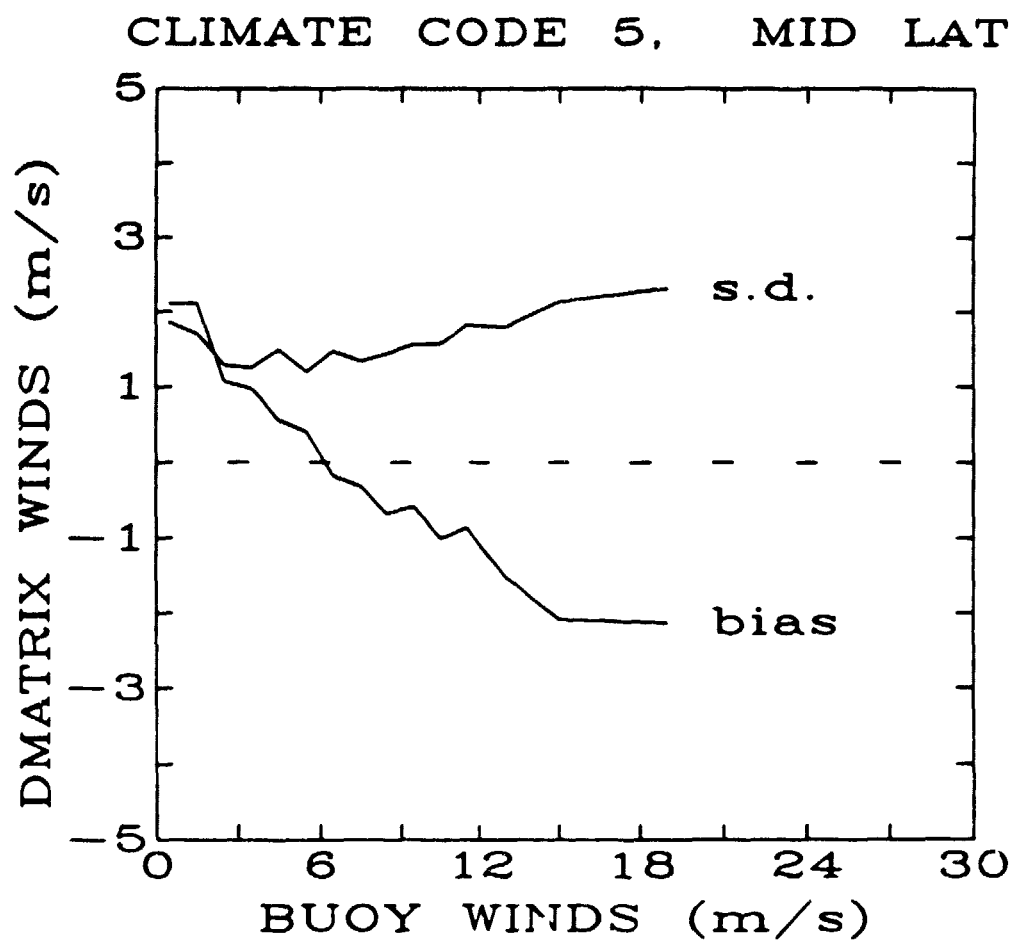
Figure 10. Standard deviation and bias of the D-matrix retrieved winds plotted as a function of buoy wind speed for climate code 5.

Climate

Codes	1	2	3	4	5	6	7	8	9
1	0	0.1/1.4	0.5/0.6	—	—	—	—	—	—
2		0	—	1.2/1.8	—	—	—	—	—
3			0	—	1.9/1.6	2.0/1.5	—	—	—
4				0	1.4/1.2	—	0.8/2.1	—	—
5					0	—	—	0.4/1.3	1.9/2.9
6						0	—	0.5/1.5	—
7							0	—	1.3/1.9
8								0	—
9									0

Average (m/s) $/$ Standard Deviation (m/s)

Table 6.   Average and standard deviation of the wind speed discontinuity across the D-matrix zonal boundaries.

The fact that the accuracy of the SSM/I wind speed retrievals deteriorates rapidly in areas where rain and heavy cloud cover are found, severely limits the ability of this instrument to map the wind field in and around typhoons, hurricanes and tropical storms. Figure 11 shows the rain-flagged areas of typhoon Wynne as it appeared on July 25, 1987 at approximately 2040Z. According to aircraft reconnaissance data collected by the Air Force/Navy Joint Typhoon Warning Center, the rain-flag 3 area outline corresponds roughly to the 25 m/s wind speed radius of this storm which had visually observed winds as high as 60 m/s near its center.

In concluding this section, it should be noted that two and possibly three serious limitations of the 9-version original D-matrix algorithm warrant investigation of an alternate algorithm. As will be shown in the next section, both the high wind bias and zonal discontinuity problems can be partially solved using a D-matrix type algorithm while meeting the ± 2 m/s accuracy specification in an "average" sense.

7. Alternate Wind Speed Algorithm

A single D-matrix algorithm, valid at all latitudes and during all seasons was developed and found to meet the ± 2 m/s accuracy specification under rain-free conditions. This global wind speed algorithm was developed using 100 randomly selected SSM/I buoy match-ups from each of the 9 climate codes. Out of this 900 point data set, only the 708 which were rain-flagged either 0 or 1 were retained and used to develop the new algorithm. In this way, the global algorithm was based on data from types of weather systems where accurate wind speed retrievals were likely while at the same time being made somewhat tolerant of rain.
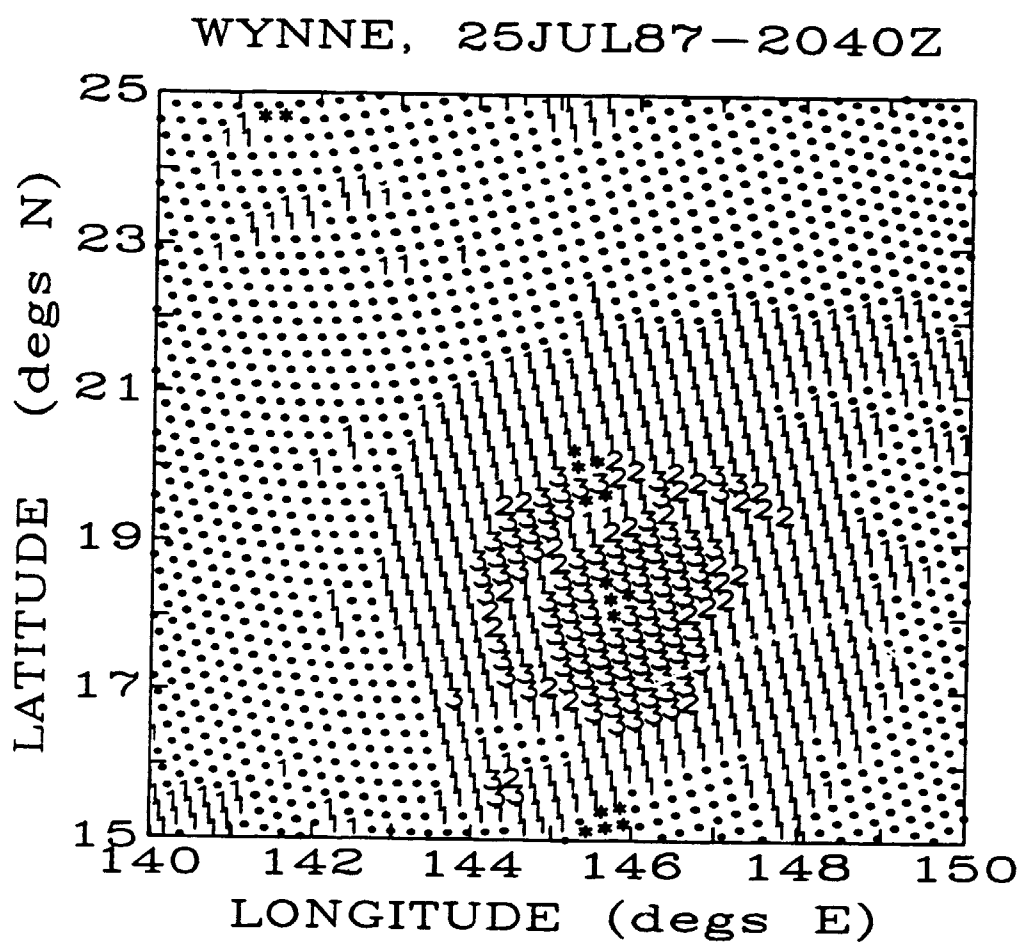
WYNNE, 25JUL87—2040Z

Figure 11. Rain–flagged areas of typhoon Wynne on 25 July 1987. The dots and asterisks indicate rain–flag zero areas and land (Mariana Isles) respectively. The numbers 1, 2, and 3, correspond to rain–flags 1, 2 and 3.

Coefficients for the global algorithm were generated using a weighted linear regression [Draper, et al., 1981] of the buoy wind speeds on the coincident SSM/I brightness temperatures of $TB(19V)$, $TB(22V)$, $TB(37V)$, and $TB(37H)$. Note that $TB(19V)$ has been used to construct the global algorithm instead of the ERT suggested $TB(19H)$; a change that resulted in slightly more accurate retrievals. The weights used in the regression were set equal to one over the square root of the wind speed density function (see Figure 1), evaluated at the particular buoy wind speed. This type of weighting has the effect of making all wind speed ranges equally important in the creation of the new algorithm. In contrast, the unweighted regression used previously tends to emphasize those wind speed ranges where there is a lot of data and de-emphasize the ranges where little data was collected. This is precisely why the original D-matrix performed well near the global average wind speed of 7 m/s and performed poorly (both in terms of SD and bias) in the high (>15 m/s) range.

Performance of the alternate global D-matrix algorithm under rain-free conditions is shown in Figure 12. The data used in this figure is comprised of withheld data taken from all 9 of the original D-matrix climate codes. From Figure 12, the retrieval SD is found to be 2.0 m/s which meets the ± 2 m/s accuracy specification.

Although the regression line in Figure 12 shows slight errors in bias and slope, true performance of the alternate global wind speed algorithm under rain-free conditions is indicated by the "interpreted" residual plot shown in Figure 13. Comparison of Figure 13 with Figure 10 shows that much of the high wind speed bias associated with the original D-matrix retrievals has been removed by the weighted regression technique.

The sensitivity of the global wind speed algorithm to rain has not improved significantly as revealed by the interpreted residual plots shown in Figures 14 and 15. The global
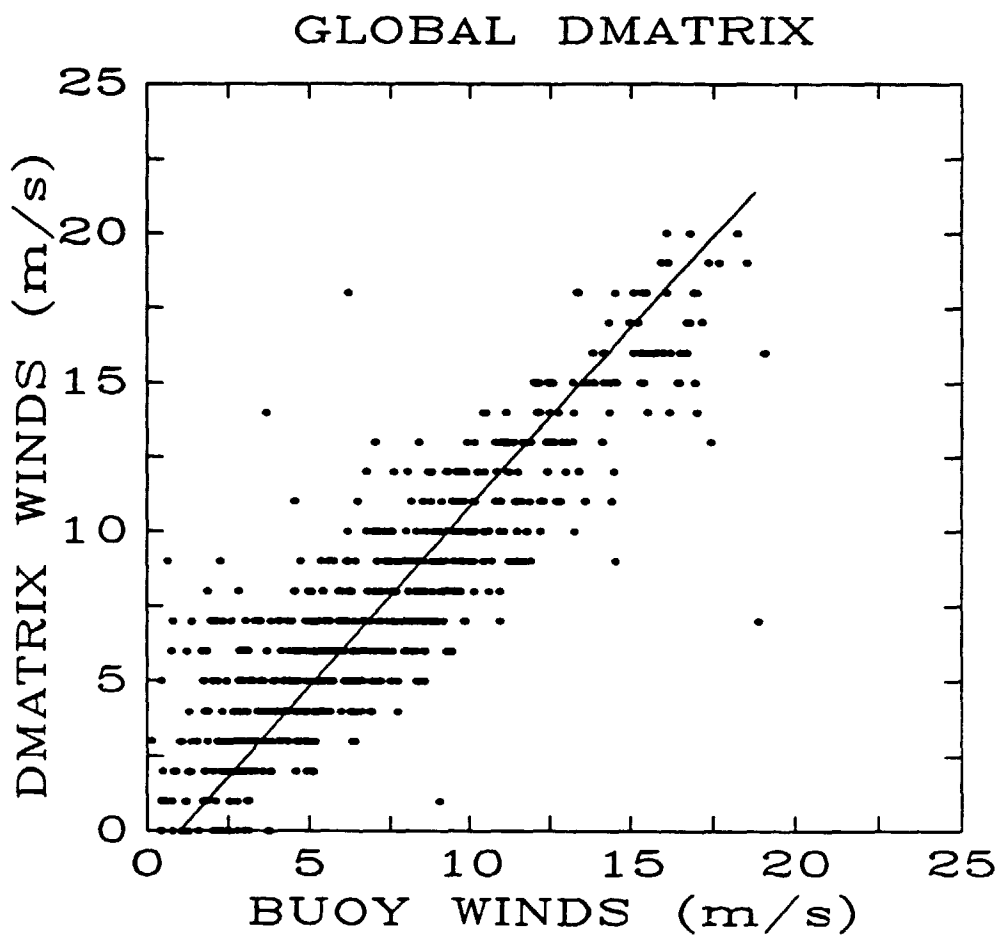
Figure 12. Performance of the global D-matrix algorithm. Bias = −1.1 m/s, slope = 1.2, S.D. = 2.0 m/s. corr (R) = 0.88, # obs = 708.
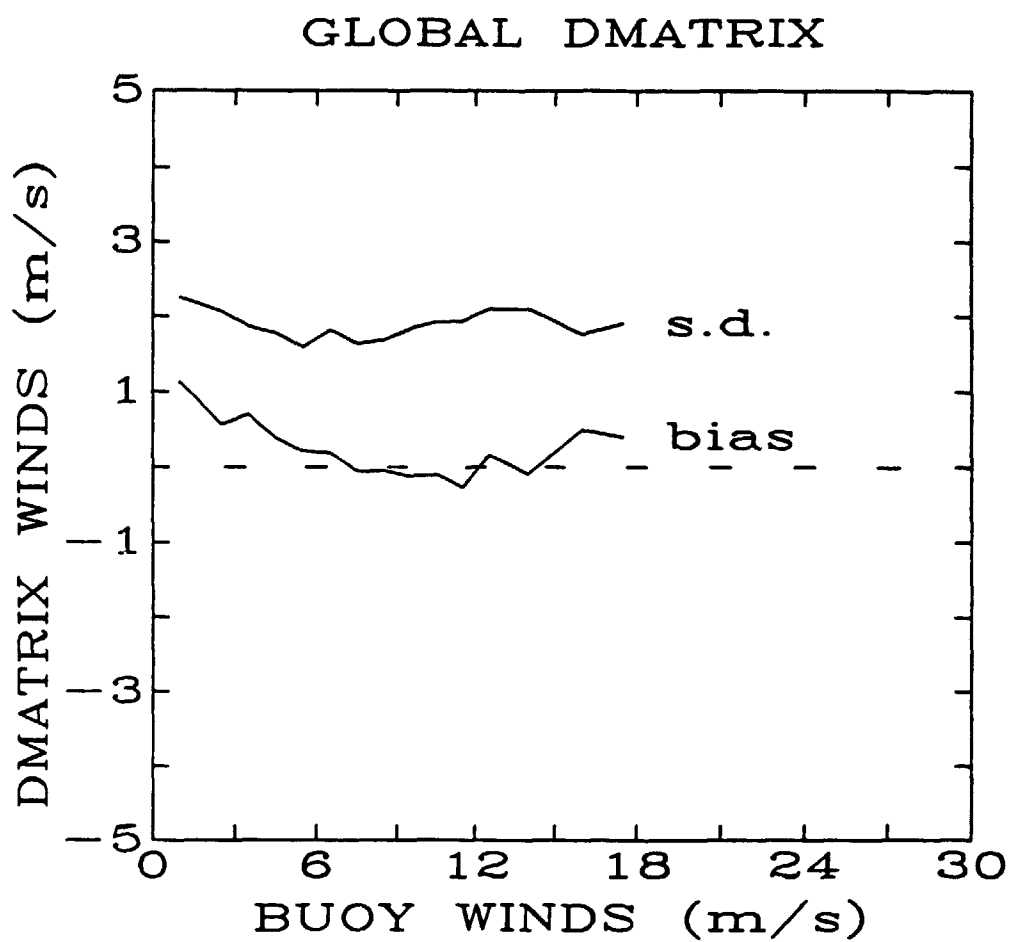
Figure 13. Standard deviation and bias of the global D-matrix retrieved winds plotted as a function of buoy wind speed.

GLOBAL DMATRIX

Figure 14.   Standard deviation and bias of the global D-matrix retrieved winds plotted as a function of the rain-flag, $(TB37V - TB37H)$.

GLOBAL DMATRIX

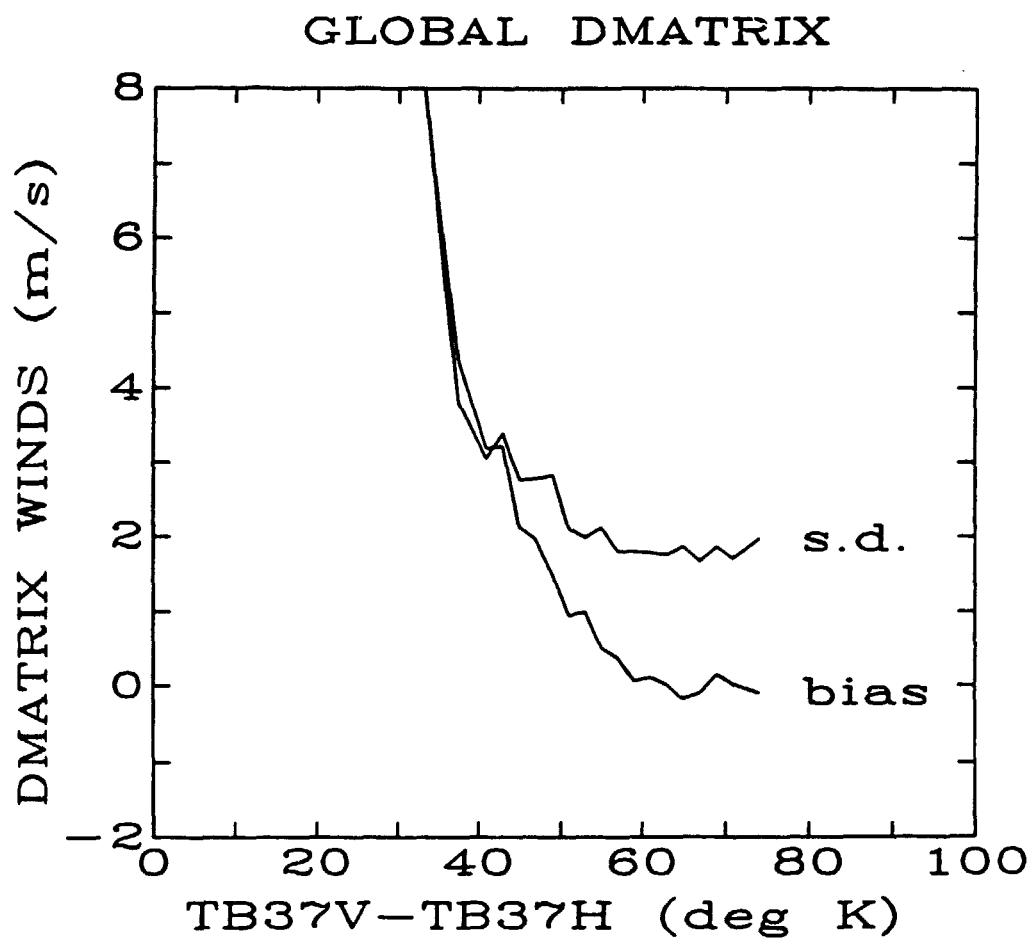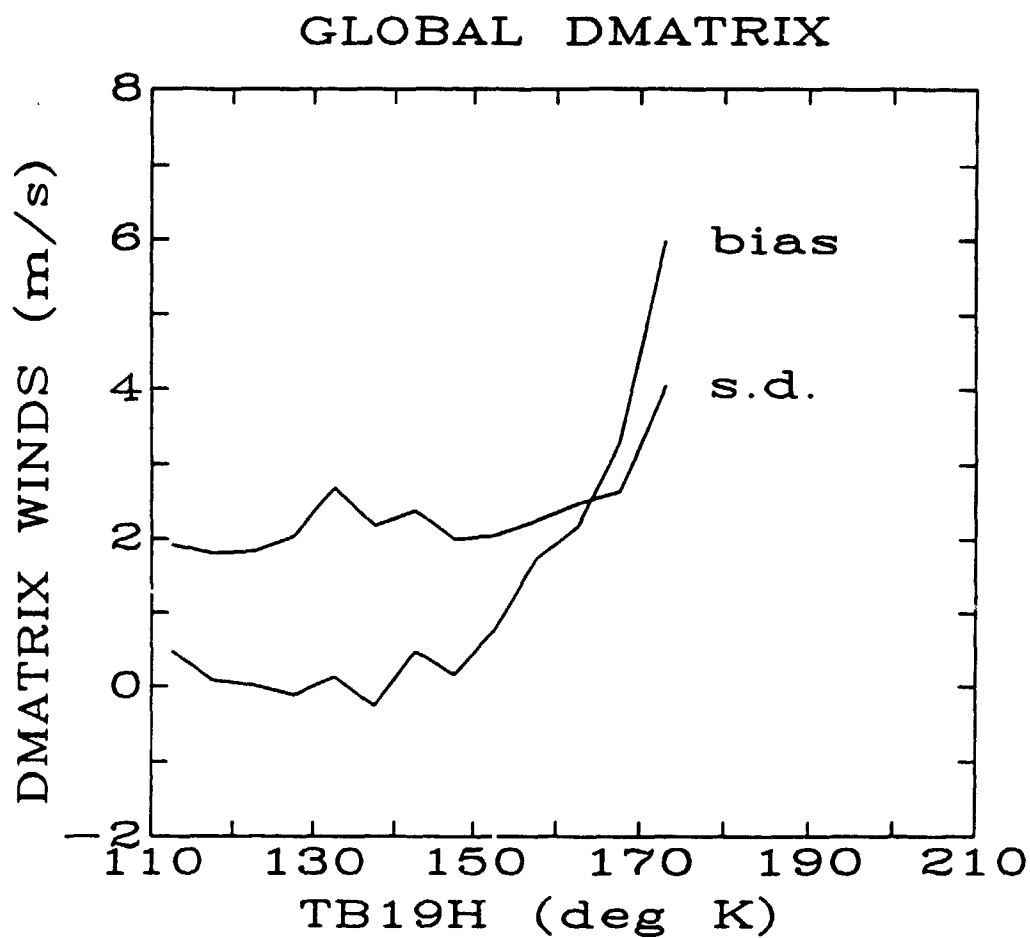Figure 15.   Standard deviation and bias of the global D-matrix retrieved winds plotted as a function of the rain-flag, $TB19H$.

D-matrix performance on a data set containing SSM/I buoy pairs that were rain flagged either 1, 2 or 3 is shown in Figure 16. The fact that a fair number of the retrievals are quite good is expected since the global D-matrix algorithm was constructed using data that was rain-flagged either 0 or 1. Figure 16 shows that the retrievals are typically biased high and the correlation coefficient of 0.27 indicates that the global wind speed algorithm performs poorly in rain as did other special rain D-matrix algorithms that were tested [Hollinger, et al., 1988]. It should be pointed out that 45 of the data points used to make Figure 16 do not appear in the plot because the D-matrix values were above 50 m/s.

Knowing what SSM/I channels are most important in the retrieval of wind speeds aides in the construction of new algorithms and indicates what retrieval accuracies are possible should an SSM/I channel become inoperative. To this end, the rain-flag 0 and 1 data points from the 900 point data set previously described were used to create the best global multichannel regression algorithms where the number of channels varied from 1 to 5. The results are summarized in Table 7 where the SD shown indicates the relative retrieval accuracy. It is interesting to note that the best 4-channel algorithm does not use the same four channels as the original D-matrix algorithm. This is why the proposed global algorithm uses $TB(19V)$ instead of the $TB(19H)$ channel selected for the original D-matrix algorithm. If $TB(19H)$ had been chosen instead of $TB(19V)$, the performance would have been slightly worse with an SD of 2.1 m/s under rain-flag zero conditions. As in the original algorithm, the alternate global algorithm also uses the 4-channel D-matrix since it represents a good compromise between calculation efficiency and retrieval accuracy.

Should one of the four selected channels become inoperative, a 3-channel or 4-channel algorithm can be constructed which would perform as indicated in Table 8. All algorithms in this table were generated from the same data set used to make the global algorithm.
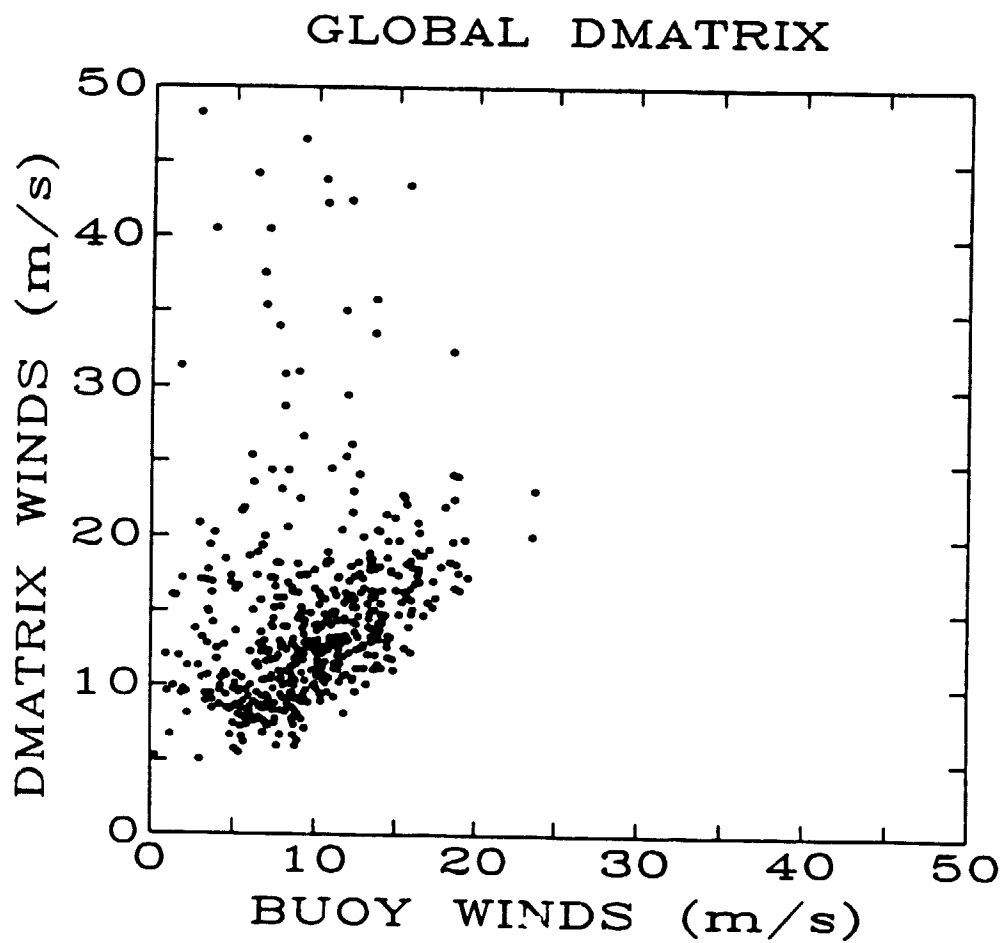
Figure 16. Performance of the global D-matrix algorithm under rain–flag 1, 2, and 3 conditions. S.D. = 8.0 m/s, corr (R) = 0.27, # obs = 525.

Number of Channels	COEFFICIENTS						S.D.
	CON	19V	19H	22V	37V	37H	
1	44.38	—	—	-0.1495	—	—	5.0
2	195.07	—	—	—	-1.5341	0.9144	2.5
3	237.57	0.2613	—	—	-2.0413	1.0092	2.3
4	147.90	1.0969	—	-0.4555	-1.7600	0.7860	2.0
5	148.25	1.0233	0.0678	-0.4692	-1.6859	0.7371	2.0

Table 7. Coefficients and relative performance of the best global multichannel D–matrix algorithms.

Algorithm ID	(3-Channel Algorithms) Coefficients						S.D.
	CON	19V	19H	22V	37V	37H	
1	198.66	X	—	0.0072	-1.5642	0.9227	2.4
2	237.58	0.2613	—	X	-2.0413	1.0092	2.3
3	-47.46	0.8133	—	-0.6816	X	0.2988	3.3
4	-113.06	1.8278	—	-1.1173	0.0419	X	3.7
	(Revised 4-Channel Algorithms)						
5	165.86	X	0.7208	-0.4729	-0.9091	0.2983	2.1
6	213.29	1.0437	-0.5325	X	-2.5612	1.3443	2.3
7	93.68	-0.1989	1.1056	-0.7511	X	-0.1703	2.5
8	124.65	0.1256	0.9607	-0.7236	-0.5050	X	2.3

"X" = Lost Channel

Table 8. Global wind speed algorithms which can be used if the SSM/I loses a channel.

Although the D matrix wind speed retrievals meet specifications under rain free conditions, some have suggested the use of iterative wind speed algorithms, mostly as a means of obtaining more accurate retrievals in and around typhoons, hurricanes and tropical storms. Unlike the D-matrix algorithm, the iterative algorithms are based on a physical model which accurately predicts the effect that both wind and rain have on the measured brightness temperature. Since the rain-dependence is known, its contribution to the total brightness temperature can be effectively subtracted out making a more accurate wind speed retrieval possible. There is little doubt that these more sophisticated algorithms would improve retrieval accuracy in rain-free and light rain conditions however, any wind speed algorithm which tries to retrieve winds in these storms from the SSM/I data is likely to fail for at least two reasons. The first reason, which was already discussed, is the fact that microwave radiation emitted from the ocean surface contains information about the wind speed and must pass through the water laden atmosphere before being measured by the SSM/I. If this wind speed signature is attenuated to a level below the SSM/I instrument noise then accurate wind speed retrievals are no longer possible. The rain rate above which accurate SSM/I wind speed retrievals are unlikely, irregardless of the algorithm, seems to be in the 0-5 mm/hr range. A second limitation to wind speed retrieval accuracy in typhoons and hurricanes is the spatial resolution of the SSM/I 19, 22 and 37 Ghz channels (55, 49 and 32 km respectively). Since wind speed gradients in the core regions of a storm are typically on the order of 2 m/s per kilometer and can persist over a distance of 25 km or more, any SSM/I wind speed retrieval under these conditions would be a gross underestimation of the highest winds present in the resolution cell.

Since the SSM/I seems to be limited in its ability to obtain accurate winds in and around typhoons, hurricanes and tropical storms, alternate instruments have been

proposed such as the Split Window Microwave Radiometer (SWMR) Swift, et al., 1988. The SWMR operates in the microwave frequency range near 5 Ghz where the emission and absorption characteristics of the rain and water vapor in the atmosphere do not significantly mask the wind speed signature coming from the surface. Its design is based on the Stepped Frequency Microwave Radiometer (SFMR) [Jones, et al., 1981] which has been flown operationally aboard NOAA hurricane hunter aircraft since 1985 and has measured winds accurately in regions where rain rates exceeded 35 mm/hr. In addition, the SWMR has 5 km resolution making it considerably more suitable than the SSM/I for measuring wind speed in the high wind gradient regions.

8. Conclusions

Although wind speed retrievals from the original ERT 9-version D-matrix algorithm did not meet the accuracy specification of ± 2 m/s, regeneration of the D-matrix coefficients using standard linear regression resulted in a set of algorithms whose retrievals did meet specifications.

An alternate global D-matrix algorithm with a single set of coefficients has been developed which meets retrieval accuracy specifications and does not have the zonal discontinuity and high wind speed bias problems found in the original ERT 9-version D-matrix algorithm. Coefficients and rain-flag criteria for the global algorithm are given in Table 9.

The rain-flag criteria was revised to be more restrictive and the global algorithm now uses the four rain-flags, 0, 1, 2, and 3, which indicate retrieval accuracy SD's of < 2 m/s, 2-5 m/s, 5-10 m/s and >10 m/s, respectively. During any particular day, approximately 85% of the D-matrix retrieved ocean surface winds will have an accuracy of ± 2 m/s. The

$$SW = 147.90 + 1.0969 \cdot T_B(19V) - 0.4555 \cdot T_B(22V) +$$

$$- 1.7600 \cdot T_B(37V) + 0.7860 \cdot T_B(37H)$$

Rain Flag	Criteria	Accuracy
0	$T_B(37V) - T_B(37H) > 50$ $T_B(19H) < 165$	$< 2\ m/s$
1	$T_B(37V) - T_B(37H) < 50$ $T_B(19H) > 165$	$2 - 5\ m/s$
2	$T_B(37V) - T_B(37H) < 37$	$5 - 10\ m/s$
3	$T_B(37V) - T_B(37H) < 30$	$> 10\ m/s$

Table 9.   Specifications of the global D-matrix algorithm.

remaining 15% of the time, the scene will be rain flagged and retrieval accuracies will be worse than ± 2 m/s.

Since a majority of the scene in and around typhoons and hurricanes is rain-flagged, the SSM/I appears to have limited use for studying the wind field of these weather systems. Additionally, the spatial resolutions of the 19, 22 and 37 Ghz channels (55, 49 and 32 km) are incapable of resolving accurately any wind speeds in areas where high wind speed gradients exist. The high rain and water vapor regions of typhoons and hurricanes are identified by rain-flag the algorithm, and in this context, the position and approximate size of the storms can be monitored.

References

[1] Book, S.A., *Statistics*, p. 221, McGraw-HIll, New York, NY., 1977

[2] Draper, N.R. and H. Smith, Applied Regression Analysis, 2nd edition, p. 108, John Wiley and Sons, New York, NY., 1981.

[3] Gilhousen, D.B., "An Accuracy Statement for Meteorological Measurements Obtained from NDBC Moored Buoys," Proc. MDS '86 Marine Data Systems International Symposium, Marine Tech. Soc., New Orleans, La., 1986a.

[4] Gilhousen, D.B., M.J. Changery, R.G. Baldwin, T.R. Karl, and M.G. Burgin, "Climatic Summaries for NDBC Data Buoys," National Data Buoy Center publication, NSTL, Ms., 1986b.

[5] Hollinger, J., R. Lo, G. Poe, R. Savage, and J. Peirce, "Special Sensor Microwave/Imager User's Guide," Naval Research Labs, Washington D.C., 1987.

[6] Hollinger J.P., "DMSP Special Sensor Microwave/Imager Calibration/Validation," Naval Research Labs, Washington D.C., 1988.

[7] Hughes Aircraft Company, "Special Sensor Microwave/Imager (SSM/I) Critical Design Review," vol. 2 (Ground Segment), p. 117, 1980.

[8] Jones, W.L., P.G. Black, V.E. Delnore, and C.T. Swift, Airborne Microwave Remote-Sensing Measurements of Hurricane Allen, SCIENCE, 214, 274-280, 1981.

[9] Liu, W.T. and T.V. Blanc, The Liu, Katsaros and Businger (1979) Bulk Atmospheric Flux Computational Iteration Program in FORTRAN and BASIC, Naval Research Labs Memorandum Report 5291, Washington D.C., 1984.

[10] Lo, R.C., A Comprehensive Description of the Mission Sensor Microwave Imager (SSM/I) Environmental Parameter Extraction Algorithm, Naval Research ᵀ abs

memo. report 5199, Washington D.C., 1983.

[11] Monaldo, F.M., Expected Differences between Buoy and Radar Altimeter Estimates of Wind Speed and Significant Wave Height and their Implications on Buoy–Altimeter Comparisons, J. Geophys. Res., 93, 2285–2302, 1988.

[12] Pierson, W.J., The Measurement of the Synoptic Scale Wind Over the Ocean, J. Geophys. Res., 88, 1683–1708, 1983.

[13] Schroeder, L.C. and J.L. Sweet, Merge and Archival of SEASAT–A Satellite Data and In situ at Selected Illuminated Sites Over the Ocean, NASA Langley tech. memo., Hampton, Va., 1986.

[14] Swift, C.T., R.L. Berstein, P.G. Black, and Harris Corporation, Split Window Microwave Radiometer (SWMR), OSSA-1-88, proposal submitted to NASA, Washington, D.C., January 1988.

[15] Ulaby, F.T., R.K. Moore, and A.K. Fung, Microwave Remote Sensing Active and Passive, vol. 3, p. 1440–1467, Artech House, Norwood, Ma., 1986a.

[16] Ulaby, F.T., R.K. Moore, and A.K. Fung, Microwave Remote Sensing Active and Passive, vol. 3, p. 1649–1657, Artech House, Norwood, Ma., 1986b.